



# Review of in-situ process monitoring and in-situ metrology for metal additive manufacturing



Sarah K. Everton<sup>a,b,\*</sup>, Matthias Hirsch<sup>a</sup>, Petros Stravroulakis<sup>a</sup>, Richard K. Leach<sup>a</sup>, Adam T. Clare<sup>a</sup>

<sup>a</sup> Department of Mechanical, Materials and Manufacturing Engineering, University of Nottingham, University Park, Nottingham NG72RD, United Kingdom

<sup>b</sup> Manufacturing Technology Centre, Ansty Park, Coventry CV7 9JU, United Kingdom

## ARTICLE INFO

### Article history:

Received 13 November 2015

Received in revised form 20 January 2016

Accepted 21 January 2016

Available online 23 January 2016

### Keywords:

Process monitoring  
Additive manufacturing  
Quality assurance  
Defect detection

## ABSTRACT

Lack of assurance of quality with additively manufactured (AM) parts is a key technological barrier that prevents manufacturers from adopting AM technologies, especially for high-value applications where component failure cannot be tolerated. Developments in process control have allowed significant enhancement of AM techniques and marked improvements in surface roughness and material properties, along with a reduction in inter-build variation and the occurrence of embedded material discontinuities. As a result, the exploitation of AM processes continues to accelerate. Unlike established subtractive processes, where in-process monitoring is now commonplace, factory-ready AM processes have not yet incorporated monitoring technologies that allow discontinuities to be detected in process. Researchers have investigated new forms of instrumentation and adaptive approaches which, when integrated, will allow further enhancement to the assurance that can be offered when producing AM components. The state-of-the-art with respect to inspection methodologies compatible with AM processes is explored here. Their suitability for the inspection and identification of typical material discontinuities and failure modes is discussed with the intention of identifying new avenues for research and proposing approaches to integration into future generations of AM systems.

© 2016 The Authors. Published by Elsevier Ltd. This is an open access article under the CC BY license (<http://creativecommons.org/licenses/by/4.0/>).

## Contents

1. Introduction	431
2. AM terminology	432
3. The industrial pull for in-situ measurement	432
4. Standardisation of AM	432
5. Review of in-situ methods	433
5.1. Powder bed fusion	433
5.1.1. Laser-PBF	434
5.1.2. Electron beam-PBF	437
5.2. Directed Energy Deposition	438
5.2.1. Powder-DED	438
5.2.2. Wire-DED	440
5.3. Other potential NDT processes	441
6. The underpinning metrology challenge: future direction	442
7. Conclusions	443
Acknowledgements	443
References	443

## 1. Introduction

Additive manufacturing (AM) has matured rapidly in recent years due to development of AM processes and materials and a greatly increased understanding of the underlying design philosophies. As a

\* Corresponding author at: Department of Mechanical, Materials and Manufacturing Engineering, University of Nottingham, University Park, Nottingham NG72RD, United Kingdom.

E-mail address: [sarah.everton@nottingham.ac.uk](mailto:sarah.everton@nottingham.ac.uk) (S.K. Everton).

result of these developments, commercial exploitation of AM has been seized by industrialists across many manufacturing sectors. This rapid uptake of AM is evidenced annually in the Wohlers Report; an annual compendium of commercial activity relating to AM. In the latest issue, the 2014 AM services market was reported to have grown by 38.9% from 2013, to reach \$2.015 billion [1]. The interest, therefore, in technologies falling under the blanket term of AM persists and underpinning technologies which facilitate the accelerated improvement of these is becoming an important research area in its own right.

While current AM machine tools are greatly improved from early versions, many of the same problems identified by early researchers in the 1980s (porosity, cracking, thermal management issues, material supply issues) persist. This is largely attributable to a lack of in-process monitoring and closed loop control algorithms used to manage machine operation. This AM monitoring deficit is somewhat at odds with the advances commonly reported in the more established area of conventional machining, where the methodologies across platforms are near standardised and machine makers share approaches to common problems (see [2] for a review on machine tool controllers). Martin's review on machine tool condition monitoring and diagnostics, while dated, highlights the maturity of machine tools which are capable of assessing and adapting their performance based on feedback collected from sensors [2]. The capability of in-situ process monitoring and in-situ metrology for AM technologies remains low and is the subject of significant ongoing research activity.

The use of Failure Mode and Effect Analysis (FMEA) tools by large manufacturers highlights the lengths that will be taken to ensure all aspects within the manufacturing space are controlled. Undertaking FMEA for a process relies on practitioners collecting process data relating to previous sources of error and phenomena that can potentially lead to failure. In order to achieve a greater understanding of the process, process data capture and analysis must be undertaken. Early attempts to apply this FMEA approach to AM [3], serve to show the importance of gathering data in process from which predictive part performance can be inferred.

Process or condition monitoring within conventional machine tools depends upon force, position and acoustic sensing. Data gathered here in-process is now commonly processed in real-time to affect an 'on-the-fly' response in machining strategy. In order to achieve a similar capability in AM systems, a new range of sensors (or repurposing of existing sensor technology) and means of incorporating them into additive tools will be required. The temporal opportunity and the environment in which parts must be interrogated in-situ present significant challenges to researchers in this field. However, several researchers have tackled these challenges with some success and have produced demonstrable technologies, capable of acquiring useful data for informing process capability without the need for ex-situ analysis.

Several AM review papers have been produced by leaders in the field which extol the merits and the state-of-the-art of systems, materials, design and usage. Early reviews were undertaken by Kruth who published an overview of machine tool progress in 1991 [4]. Widely regarded for his work in materials, applications and machine development for AM processes, Kruth et al. have published reviews in many of these areas. Highlighting the need for this review, the fundamental mechanisms of "defect" or material discontinuity formation within powder bed processes have been identified previously by Kruth et al. [5]. In addition, key reviews have been published in the area of applications and opportunities for AM techniques; these have centred around biomedical [6,7] aerospace [8], tooling [9] and general manufacturing [10]. Part quality and homogeneity (inter-build, inter-batch, inter-machine) are often identified as shortfalls of AM in these reviews hence there is a need to conduct research to address this.

Several papers published recently in this journal also highlight the challenges for AM, regarding quality control. Sercombe et al. investigated failure mechanisms within laser powder bed fusion components, concluding that an improvement in build quality is required to

minimise localised stresses and reduce component failure at these sites [11]. Cooper et al. recognised that the increased design complexity allowed by manufacture by AM, necessitates non-destructive evaluation of internal component geometries [12]. Qiu et al. bring our attention to lack-of-fusion porosity, common at inter-layer boundaries [13]. In each of these cases, an in-situ monitoring method could be implemented. This paper builds on a review previously carried out [14] and draws together research in the area of in-situ analysis for AM processes, highlighting the key technologies for process control in metal based AM systems.

## 2. AM terminology

AM is defined in the American Society for Testing and Materials (ASTM) standard F2792 as "the process of joining materials to make objects from 3-D model data, usually layer upon layer, as opposed to subtractive manufacturing technologies" [15]. Historically, a number of terms have been used to refer to the various AM processes with each manufacturer adopting its own term; in some cases a registered trademark. In this review, the naming convention agreed in the aforementioned standard will be employed. For reference, terms are outlined in Table 1, adapted from the ASTM classifications [16]. A comprehensive introduction to AM technologies is available from Gibson et al. [17].

## 3. The industrial pull for in-situ measurement

A 2012 report issued by the UK AM special interest group (SIG) titled "Shaping our national competency in additive manufacturing" highlights a lack of robust AM processes as a key barrier to the adoption of AM in the UK. A critical factor to this deficiency is the limited control and monitoring of processes, in-situ [16]. In-situ data acquisition, in order to enable closed-loop control and detection of material discontinuities, was similarly highlighted as a key barrier to implementation and as a priority area for research and development in the US National Institute of Standards and Technology 2013 "Measurement science roadmap for metal-based additive manufacturing" [18].

In the UK, a steering group has since been assembled comprising representatives from prominent users of AM in the private and public sectors [19]. This steering group is responsible for establishing a UK national strategy for AM. A positioning paper has been published initially discussing the challenges for industrial exploitation of AM. Amongst these, the need for in-process monitoring and control is again highlighted [20].

A summary of the in-situ monitoring and closed-loop feedback modules currently available from prominent AM machine manufacturers is shown in Table 2. As can be seen, many manufacturers now offer additional modules which can be added onto the basic AM machine, although in many cases, the data generated is stored but not analysed in real-time for closed-loop feedback.

## 4. Standardisation of AM

The specification standards landscape regarding non-destructive testing (NDT) for AM is currently convoluted, although urgent need for AM standards has catalysed the co-operation between the International Organization for Standardization (ISO) and ASTM for the first time with the formation of joint groups between ISO TC261 and ASTM F42. This collaboration will enable the joint development of AM standards in the areas of 'Terminology', 'Standard test artefacts', 'Requirements for purchased AM parts', 'Design guidelines', 'Standard Specification for Extrusion Based Additive Manufacturing of Plastic Materials', 'Standard practice for metal PBF to meet rigid quality requirements', 'Specific design guidelines on PBF', 'Qualification', 'Quality assurance and post processing of PBF metallic parts' and more importantly in this case, 'Non-destructive testing for AM parts' [21].

**Table 1**  
AM terminology.

ASTM classification	Term used in this article	Commercial name	Machine manufacturer
Powder bed fusion (PBF)	Laser-PBF	Direct metal laser sintering (DMLS)	EOS
		LaserCUSING	Concept Laser
		Selective laser melting (SLM)	Matsuura
		Direct metal production (DMP)	Phenix (3D systems)
		Selective laser melting (SLM)	Renishaw
		Selective laser melting (SLM)	Realizer
		Laser metal fusion (LMF)	Sisma Group
		Selective laser melting (SLM)	SLM Solutions
		Electron beam melting (EBM)	ARCAM
		Direct metal deposition (DMD)	POM
Directed energy deposition (DED)	Powder-DED	Laser engineer net shaping (LENS)	Optomec
		Laser consolidation	Accufusion
		Laser deposition	Irepa Laser
		Laser deposition	Trumpf
		Laser deposition	Huffman
		Electron beam direct melting (EBDM)	Sciaky
		Shape metal deposition (SMD)	Other
	Wire-DED		

The standardisation process is on-going although the following standards documents have been released in the UK by British Standards Institute (BSI), in close co-operation with ISO and ASTM:

- BS ISO/ASTM 52921:2013 – Standard terminology for additive manufacturing. Coordinate systems and test methodologies [22].
- BS ISO/ASTM 52915:2013 – Standard specification for additive manufacturing file format (AMF) Version 1.1 [23].
- BS ISO 17296-4:2014 – Additive manufacturing. General principles. Overview of data processing [24].
- BS ISO 17296-3:2014 – Additive manufacturing. General principles. Main characteristics and corresponding test methods [25].
- BS ISO 17296-2:2015 – Additive manufacturing. General principles. Overview of process categories and feedstock [26].

## 5. Review of in-situ methods

The following sections detail the work carried out to date on in-situ inspection of metal AM processes, covering first PBF and then DED processes. Finally, other NDT processes, that are yet to be trialled in-situ, but that have been identified as being potentially suitable for in-situ inspection, are reviewed. For each section, a brief introduction is given to the process and the measurement environment as well as the type of material discontinuities that commonly occur during processing. An overview of research in the area is then given and discussed.

### 5.1. Powder bed fusion

Powder bed fusion (PBF) includes processes which utilise a laser or electron beam energy source. The two technologies are inherently similar in their operation, repeatedly spreading a layer of loose powder on the build platform which is then melted and fused with the previous

layer [27], before the platform is lowered and the cycle repeated. The different energy sources necessitate different operating atmospheres. In the case of the laser systems, an inert atmosphere, usually nitrogen or argon, is required. The electron beam process requires a near vacuum [28], as the mean free path of electrons is very short; an added bonus is that there is no oxygen to cause oxidation. During melting, a partial pressure of helium gas is introduced at approximately  $10 \times 10^{-2}$  mbar and directed at the build area, in order to enhance heat transfer and cooling of the component [29]. Reviews of both the laser-PBF [30] and electron beam-PBF processes [31] have been carried out and provide further detail of the process variants.

PBF processes have a great number of input parameters which affect the quality of the final product. For the laser-PBF process, Van Elsen lists over fifty [32] and experimental studies have been widely undertaken to assess the effects of energy density, traverse speed and hatch spacing. These input parameters are linked with optimisation of build quality in order to reduce observable material discontinuities. A wide range of material discontinuities are known to occur during AM processing, the most common of which (termed pores) are voids that are situated in the bulk of the fused material either in between layers (elongated pores [33]) or within the layer (gas pores [34]). Attar et al. reported that gas pores form in laser-PBF due to partially un-melted powders with low laser power but with constant energy input. It was shown that lower laser had a drastic impact on pore formation. Conversely, over-melting can lead to increased turbulence within the meltpool and excessive evaporation, resulting in the formation of gas pores within the bulk material [35]. Tammis-Williams et al. built Ti6Al4V structures by electron beam-PBF and used X-ray computed tomography (XCT) to show that the formation of voids corresponds directly to the hatching/scanning regime and processing parameters used [36]. Similarly, Antonyamy et al. have investigated grain structure and texture development of Ti6Al4V parts produced with electron beam-PBF and

**Table 2**  
In-situ measurement ‘modules’ available from AM machine manufacturers and measurement specialists.

AM process	Machine manufacturer	‘Module’ name	Failure mode monitored	Parameter altered	Equipment
EB-PBF	Arcam	LayerQam™	Porosity	N/A	Camera
L-PBF	B6 Sigma, Inc. (specialist)	PrintRite3D® INSPECT™	Unknown	N/A	Thermocouple and high-speed camera
	Concept Laser	QM melt pool	Melt pool monitoring	Laser Power	High-speed CMOS-camera
	EOS	N/A	Unknown	N/A	Camera
DED	DEMCON	LCC 100	Melt pool monitoring	Laser Power	Camera
	DM3D Technology	DMD closed-loop feedback system	Melt pool monitoring and build height	Laser Power	Dual-colour pyrometer and three high-speed CCD cameras
	Laser Depth	LD-600	Depth measurement	Laser Power	Inline coherent imaging
	Promotec	PD 2000	Melt pool monitoring	N/A	CMOS-camera
		PM 7000	Melt pool monitoring	N/A	1D photo detector
	Stratronics	ThermaViz system	Melt pool temperature	Laser Power	Two-wavelength imaging pyrometer

concluded that the skin scan (as part of the scan strategy) produces distinctly different grain structures compared to the bulk of the material [37], which can also lead to the formation of the types of material discontinuities discussed above.

Other material discontinuities have been observed in laser-PBF manufacture; Attar et al. reported on elongated porosities as well as unmelted particles in the manufacture of commercially pure titanium powder [34]. It was shown that the processing parameters, such as insufficient laser power and hence unbalanced viscosity of the liquid pool, were the main reasons for the formation of these discontinuities. ‘Balling up’ of the powder has been observed in a high laser power environment, where the powdered material forms spheres that exceed the layer thickness, due to a presence of oxygen (>0.1%) in the build chamber leading to oxidation. Subsequent layers amplify this discontinuity due to the resulting powder layers being non-uniform. This behaviour has been seen in stainless steel, iron and nickel based powders, shown in Table 3 [38,39]. Li et al. have shown that an increase of the oxygen content in the laser-PBF apparatus to 10% resulted in oxidation of the powder upon solidifying [38]. Gu et al. showed that similar balling of stainless steel powders can be observed in a low power environment, where the laser power is insufficient to melt the powder fully [39]. Partial re-melting of the surface has successfully been used in combating balling of the laser-PBF processed components. Residual stresses have also been observed in laser-PBF components; the chosen hatching regime plays a major role in the residual stress development of a part, with resulting stresses concentrated perpendicular to the scan direction [40]. A method to reduce residual stress in parts produced is to compensate for the stark temperature gradient by heating the build platform [41]. Furthermore, it has been shown that a change in scan strategy affects the cracking behaviour arising from these stresses, by altering the cooling rate behaviour [42]. The material discontinuities discussed above are summarised in Table 3.

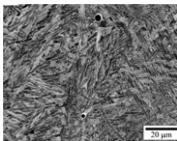
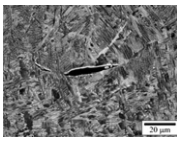
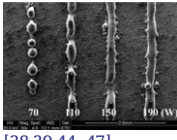
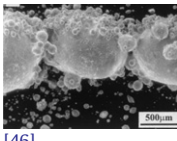
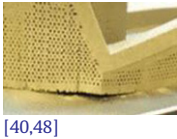
Many non-destructive, in-situ monitoring methods for laser-PBF and electron beam-PBF have been explored. Thermographic and visual monitoring methods are common, but some more novel testing techniques have also been investigated. This research is summarised here, covering first laser-PBF and then electron beam-PBF studies. A useful overview of terminology used to describe sensors for process monitoring is given by Purtonen et al. in their paper covering the monitoring and adaptive control of laser processes [49] and as such, will not be detailed here.

#### 5.1.1. Laser-PBF

Much of the early work looking at in-situ inspection of laser PBF has utilised an in-line camera based set-up, including that of Berumen et al. [50]. Electromagnetic radiation emitted by the meltpool was transmitted through the scanhead and a semi-transparent mirror used to transmit an image to a high speed camera and a photodiode, as shown schematically in Fig. 1(a). The camera measured the dimensions of the meltpool and the photodiode measured the mean radiation emitted. In this instance, solely the active laser-PBF build area was monitored, allowing a resolution of 10  $\mu\text{m}$  per pixel and limiting the image data requirement to 636 MB/s at 16,666 frames/s (from 75.1 GB/s with image capture of the full bed). Investigations showed that temperature gradients across the build area could be identified by the photodiode sensor alone, although for full control, a camera with high temporal and local resolution of the meltpool is optimal; an example output is also shown in Fig. 1(b). Closed-loop feedback could be added to stabilise the meltpool and keep the temperatures within a pre-defined window (a priori knowledge is required); this approach reduces the occurrence of over-melted zones and resulting gas pores. This method has been patented and is exclusively licenced by machine manufacturer Concept Laser [51].

Subsequently, Clijsters et al. went on to develop a system that includes a data processing algorithm to identify additional material

**Table 3**  
Summary of PBF discontinuities.

Material discon.	Photo	Description	Typical sizes
(Gas) pores	 [33,36]	Entrapped gas pores within the bulk of the material. Material dependent.	~9.9 $\mu\text{m}$ (electron beam-PBF) 5–20 $\mu\text{m}$ (laser-PBF)
(Elongated) pores	 [33,36,43]	Lack of fusion pores in between layers of the AM process.	50–500 $\mu\text{m}$
Balling	 [38,39,44–47]	Molten material is not a flat layer, but instead creates large spherically shaped particles on the surface.	Part dependent – theoretically up to the length of the part.
Unfused powder	 [46]	The melt pool varies in size and unfused powder is present.	Satellite powder clumps: 100–150 $\mu\text{m}$ .
Cracking	 [40,48]	Cracks can be within the component or more commonly, a disconnection of the part from the baseplate is seen.	Parts on bed: residual stress in the range of materials yield strength. Parts removed from bed: deformation may occur without heat treatment or further processing.



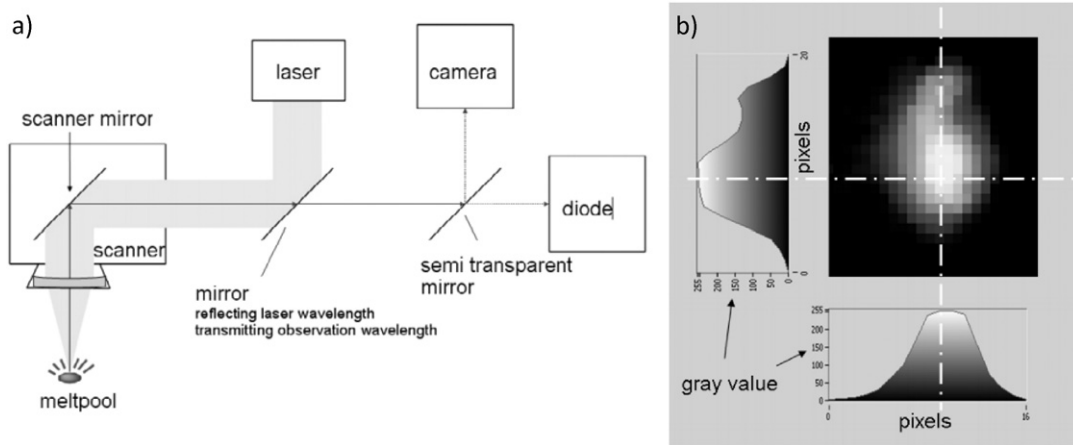


**Fig. 1.** (a) Schematic showing arrangement of photodiode and camera and (b) an example output from the camera system showing varying intensity values (right) achieved by Berumen et al. [50].

discontinuities caused by process failure and monitors the whole powder bed [35]. The melt pool monitoring system remained integrated into the optical setup of a bespoke laser-PBF machine, allowing the position of the laser relative to the powder bed to be logged in tandem with the melt pool data, creating a map. Radiation was again transmitted back through an f- $\theta$  lens, scan head and semi-reflective mirror to a beam-splitter that splits the beam towards a planar photodiode and a high speed CMOS camera, sensitive in the wavelength range of 400 nm to 900 nm. The upper bound of wavelength captured was set to 950 nm to avoid sensing the laser (1064 nm) and the lower bound set to 780 nm, above the threshold for visible light. The system returned a map of each layer with dark zones representing areas of reduced signal magnitude, due to lower thermal resistance. Algorithms are still to be developed that allow the information to be extracted from the maps automatically [52]. This camera based system, coupled with high speed image processing at a sample rate of 10 kHz to 20 kHz, has since been shown to be capable of interrogating the whole build, rather than just the melt pool itself, and can distinguish between areas of fused powder and pores. The melt pool analysis systems make use of field programmable gate array chips which enable real-time processing of melt pool images. Monitoring of ‘balling’, overheating and porosity has been trialled. The system output has been compared with XCT scans for common AM alloys, Ti6Al4V, AlSi10Mg and NiTi, and large pores (1 mm diameter) have been identified using thresholding [35]. Further work is required to allow for automated detection of process failures.

A simpler, off-line approach was trialled by Furumoto et al. who assembled a Photron FASTCAM SA5 model 1300K C2 high-speed camera onto a bespoke laser-PBF machine [53]. The camera was assembled vertically above the powder bed in order to monitor the consolidation of the metal powder during irradiation. The effect of altering powder layer thickness was successfully investigated by interpretation of camera images captured at a frame rate of 10,000 fps (10  $\mu$ s sampling time), illuminated by a metal halide lamp. The experimental set-up can be seen in Fig. 2.

Furumoto et al. have also investigated the consolidation mechanism of metal powders during processing by implementing a two-colour pyrometry system onto the machine, and using this in combination with the above set-up [54,55]. The pyrometer was used successfully to relate the consolidation phenomena with the surface temperature and to understand the solidification process of the molten powder. This work was not carried out with a view to controlling melt pool behaviour during processing through monitoring the surface temperature and as such, real-time interpretation of the data was not possible.

Pyrometry is well suited to in-situ process temperature measurement, as direct body contact with the object being measured is not required. Temperature measurement accuracy is typically  $\pm 5$  °C,

although for absolute temperature measurements, the emissivity value for the object in question must be known. Due to the simplicity of the device, pyrometry has been used to monitor laser-PBF melt pool characteristics (recording and analysing melt pool temperatures) by a number of research groups. Pavlov et al. have investigated the use of a two wavelength pyrometer (registering surface thermal radiation) in-line with the optical unit of a laser-PBF Phenix PM-100 [56]. The image in Fig. 3(a) shows 1) the laser spot size (70  $\mu$ m diameter) and 2) the pyrometer field of view (560  $\mu$ m diameter). Trials were carried out to assess the ability of the system to monitor hatch distance variation for various powder layer thicknesses and the variation of powder layer thickness. The pyrometer signals were found to differ depending on the melting strategy implemented, as this affected the powder consolidation, melting and solidification and hence the resulting structure and porosity. An example output from the pyrometer is shown in Fig. 3 (b) and an image of the corresponding build layer in (c). From the recorded data, the achieved hatch distance was grouped as low (<105  $\mu$ m), high (>120  $\mu$ m) or in a transition zone between. Layer thickness was found to affect the readings due to the heat accumulation in the previously melted layer.

Following on from the work detailed above by Pavlov et al., Doubenski et al. integrated a visual control system onto the Phenix PM-100, in order to monitor the deposition of the powder layer and to verify the position of the laser beam [57]. Illumination of the powder bed was provided by a light emitting diode (LED) ring light system,

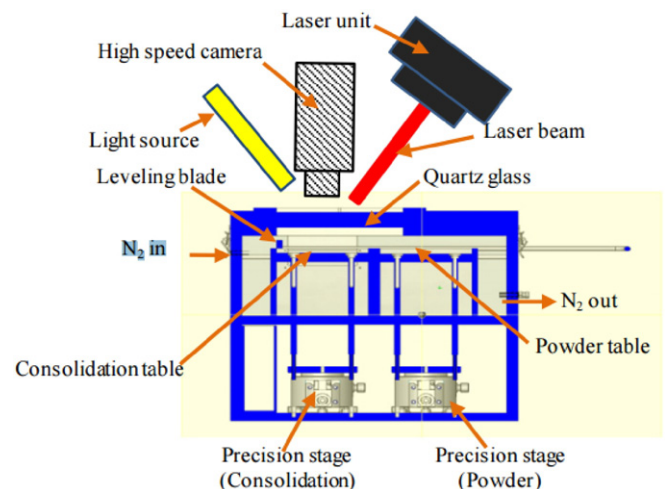


**Fig. 2.** Showing experimental set-up of high-speed camera used by Furumoto et al. [53].

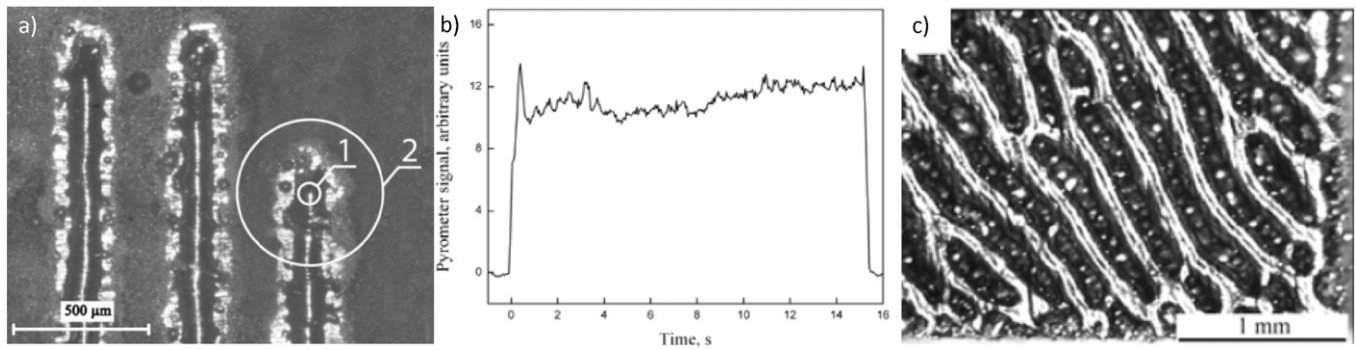


Fig. 3. (a) Image showing pyrometer field of view, (b) an example pyrometry signal and (c) an image of the corresponding layer from Pavlov et al. [56].

with a wavelength of 440 nm. This illumination scheme was designed to ensure that the intensity of the LED scattered radiation exceeded all other emittance, except in the laser impact zone. The pyrometry system was upgraded to include two InGaAs photodiodes which gave a greater field of view (1120 μm diameter), although only relative temperature readings could be recorded without accurate emissivity values. Islam et al. have also explored pyrometry in combination with a visual inspection system, although in order to investigate the causes of balling, rather than to monitor the process in real time [58]. A pyrometer with a greatly increased field of view (15 mm diameter) was utilised with a diode laser illumination selected to illuminate the bed for photography. Within the nitrogen-filled build chamber, a sheet of shielding float glass was required to protect the processing optics and inspection system; focussing the camera and pyrometer through the glass window resulted in errors which had to be accounted for through preliminary testing. Balling was found to be reduced to a minimum at heat inputs in the range  $1400 \text{ J mm}^{-3}$  to  $1700 \text{ J mm}^{-3}$  and cooling rates were not found to have any effect on balling phenomenon; the system will next be used to assess the effect of altering scanning speeds on balling.

Whilst pyrometry-based systems have been proven capable of producing useful images of the melt pool area, in order to aid understanding of the material melting and solidification process, there are no examples of pyrometry being utilised for closed-loop inspection. This is perhaps due to the limited data capture rate of pyrometers. Use of an infrared (IR) camera offers an alternative non-contact thermal measurement, at a greater capture rate and with greater accuracy. An IR camera has been used by Krauss et al. to investigate the limits for detecting pores and other irregularities caused by insufficient heat dissipation during laser-PBF processing [59]. This was done through observation of the temperature distribution of an EOSINT M270 powder bed, processing Inconel 718, using an IR camera at a long wave infrared (LWIR) wavelength band and 50 Hz sampling rate. An uncooled microbolometer detector Infratec Variocam hr head was mounted at

$45^\circ$  to the build platform, outside the germanium shielding glass in the machine window, as shown in Fig. 4(a). This arrangement allowed for a field of view of  $160 \text{ mm} \times 120 \text{ mm}$ , approximately 30% of the total build area. The inspection equipment could not be set-up inside the build chamber due to accessibility restrictions. The study aimed to identify deviations during the build process caused by drifts in process parameters or random process errors, along with detection of internal cavities and artificial flaws. It was concluded that, so long as deviations occurred at a timescale greater than 20 ms, it was possible to detect them by comparing different measurement values to predefined reference values. Circularity and aspect ratio could be used to detect deviations and drifts in the scanning unit. Additionally, material discontinuities down to  $100 \mu\text{m}$  could be detected. An example thermogram of the heat-affected zone in a sample with an artificial flaw is shown in Fig. 4(b). This externally mounted, fixed camera approach does not allow for inspection across the whole build area, although it is claimed that no additional illumination of the build area is needed. Shielding glass was again implemented to protect the camera from optical damage during laser processing and mounting the equipment externally removes any concern over optic cleanliness. It is worth noting that if integrating an IR system within an AM machine, protection from the high levels of dust or smoke produced would need to be considered as contamination can make IR equipment less accurate.

High speed cameras have been implemented for melt pool monitoring, but they can also for detection of errors and material discontinuities on a powder bed level, as Craeghs et al. have explored [60]. A camera was utilised to monitor the powder bed for inconsistencies caused by parts 'curling up', as a result of stresses within the build. These areas of raised material can damage or wear the recoater blade, interrupting the subsequent distribution of the powder layer. As seen in Fig. 5(a), the camera was mounted at an angle to powder bed axis and a simple calibration algorithm used to eliminate perspective distortion. Multiple light sources were required to provide illumination perpendicular and

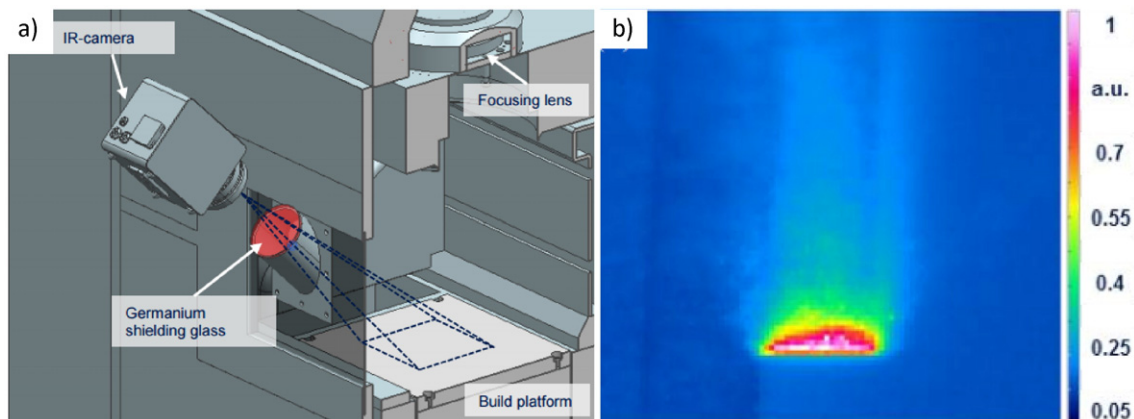


Fig. 4. (a) Schematic of equipment set-up and (b) thermogram of the heat affected zone in a sample with an artificial flaw created by Kraus et al. [59].

parallel to the recoater, and perpendicular to the build platform. Detection of this shortfall in powder distribution prior to processing is desirable, as appropriate measures can be taken to rectify the powder supply before any material discontinuities are created. An example image showing imperfections caused in the powder bed by a damaged recoater blade is shown in Fig. 5 (b).

In 2009, Kleszczynski et al. proposed a coaxial assembly for imaging of the melt pool [61]. The following year, however, the set-up had been altered to an externally mounted arrangement for monitoring an EOSINT M270, using a high speed camera. This approach was favoured as a modification of the operating system of the AM machine was not required. A SVCam-hr29050, SVS-VISTEK monochrome CCD camera system was focussed through the observation window, as shown in Fig. 6, and a Hartblei Macro 4/120 TS Superrotator was implemented to reduce perspective distortion of the build plane. A field of view of 130 mm × 114 mm was achieved, covering the small build platform used for this study. It is acknowledged that increasing the field of view to monitor the entire 250 mm × 250 mm build platform leads to a reduction in spatial resolution.

Perspective distortion was corrected using four-point homography estimation and warping with bicubic interpolation. Resolution of two 40 µm black lines, 40 µm apart on a white background was achieved at 500 mm. Diffuse lighting using matt reflectors on the back of the machine and recoater blade were found to be adequate in avoiding saturation of the camera's CCD sensor. For each layer, two images were taken — one after powder deposition and another after melting. These images were found to show voids in the powder bed, powder degradation (by comparison) and also areas where curling of unsupported structures had occurred; these elevated areas can also be identified as shown in Fig. 7(a), with detail shown in Fig. 7(b). All work was carried out manually without any integration with the EOSINT M270 itself, although coupling of the process monitoring system and the process control software was identified as desirable [62]. Subsequently, processing software has been developed to identify elevated regions across the powder bed. In order to speed up the identification process and reduce the computational load, the input CAD model is used to create a region of interest around the part, for analysis [63].

To summarise, early work in developing an in-situ monitoring system for laser-PBF concentrated on monitoring of the melt pool using in-line cameras, in combination with photodiodes and some closed-loop control of melt pool temperature was achieved. Less complex, off-line systems, which do not require machine integration, have been used to study melt pool behaviour further and have allowed a developed understanding of the balling phenomenon. Pyrometric techniques have proven popular, but the limited field of view and data capture rates have restricted the development of a closed-loop system. IR systems have shown good potential for in-situ inspection of laser-PBF processing, but have yet to be integrated into a machine. Melt pool monitoring,

along with detection of material discontinuities such as (artificial) pores, has been carried out. Imaging of the wider powder bed using high speed cameras has enabled imperfections in the powder bed due to recoater damage and areas of over-processing causing part curling to be identified, although the analysis task is largely a manual activity and again, closed-loop feedback is yet to be achieved.

### 5.1.2. Electron beam-PBF

Although the laser and electron beam-PBF processes follow approximately the same process steps, the different equipment and processing conditions provide a number of additional challenges for in-situ process inspection. For example, the electron magnetic coils used to deflect the electron beam during electron beam-PBF processing prohibit a co-axial arrangement being implemented [28] and evaporation and condensation of metal from the melt pool can lead to metallisation of the machine viewing window [64]. Processing is carried out in a vacuum, limiting the integration of inspection equipment inside the machine. Pyrometry based methods are rendered unsuitable due to the fast, transient nature of the electron-beam energy source. Instead, IR devices have been largely favoured for monitoring of electron beam-PBF processes.

Schwerdtfeger et al. equipped an Arcam A2 electron beam-PBF system with a FLIR Systems A320 IR camera with a processing resolution of 320 × 240 pixels [28]. The camera was positioned alongside the electron beam gun at a 15° angle to the bed, shielded by a zinc-selenide (ZnSe) window to protect the equipment from metallisation. A snapshot was taken after melting, before the following powder layer was raked across and when correlated with the build height, this image was compared to an optical image of a ground sample. The resolution of the IR image was limited, but a correlation with voids physically found was seen — indicating that areas of higher heat radiation correspond to material flaws. Image quality was improved by subsequent sharpening and altering of the contrast of the image. This visual imaging set-up allowed an understanding of how flaws are transferred from layer to layer as the build progresses to be developed, although an automated process would be required to progress from detection to repair through implementation of a closed loop system. Price et al. at the used a similar system to determine the repeatability of temperature measurements, build height effect on temperature profiles, transmission losses due to metallisation of sacrificial glass, molten pool emissivity, molten pool dimensions and overhanging structure thermal effects [65]. Future work will include the validation of process models to predict thermal characteristics during processing.

Rodriguez et al. incorporated an IR camera into an Arcam A2 electron beam-PBF machine, shown in Fig. 8(a), in order to analyse surface temperature profiles for each build layer [66]. Additionally, this information was then used to modify the build settings for the following layer. A FLIR Systems SC645 IR camera was selected to be integrated into the Arcam A2 based on its high resolution (640 × 480 pixels) and measurement

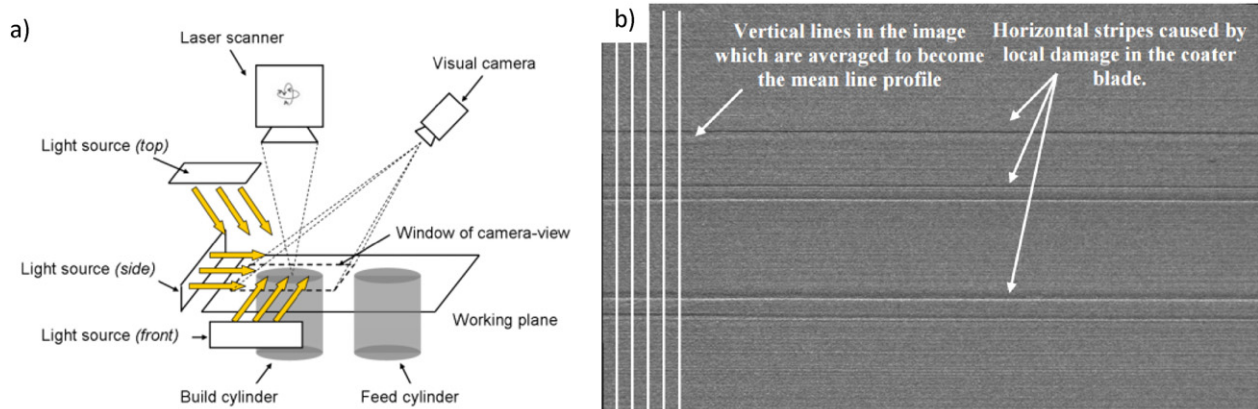


Fig. 5. (a) Visual inspection system principle and (b) example image of deposited powder bed generated by Craeghs et al. [60].



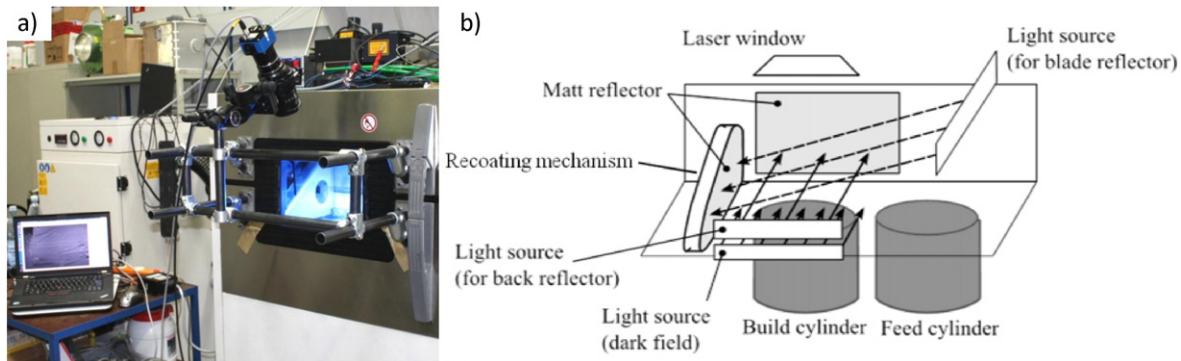


Fig. 6. (a) CCD camera set-up external to EOS M270 and (b) lighting schematic selected by Kleszczynski et al. [62].

temperature range to 2000 °C. A good number of machine modifications were required to install the IR camera, which included replacing the systems previous camera with ZnSe glass, installing a protective flap, which acts as a shutter, protecting the ZnSe window, and installing a pneumatic actuator to activate the shutter flap. The control system was also modified in collaboration with Arcam to trigger the shutter and image capture. ThermoCAM Researcher was used to analyse the images manually, measuring the emitted radiation from the surface (emission from an object, reflected emission from ambient sources and emission from the atmosphere) and converting this to a relative temperature reading. Material discontinuities caused by “over-melting” during processing could be identified from the generated IR image, shown in Fig. 8(b).

Subsequently, Mireles et al. set out to develop an automated feedback control method to maintain uniform build temperatures [67]. Rather than simply recording, archiving and then processing the images, a virtual instrument was created to perform automatic control of electron beam-PBF technology, achieve parameter modification (useful for grain size control), to attempt temperature stabilisation and to detect porosity. Parameter changes implemented to stabilise temperature resulted in part porosity, but this could be successfully detected. An improved virtual instrument has since been developed to allow for automatic control of machine parameters, using layer information to change parameters as required. Parts were detected and an average temperature stored along with data regarding part porosity, which was monitored. This stored information was useful for post-build part analysis. Further work will aim to directly access the Arcam system to avoid any delays in prompting a parameter change after the simulated user- input [68].

To conclude this section, three instances of monitoring electron beam-PBF systems using IR cameras have been found. At present, material discontinuities caused by over-melting can be identified and the general location fed back to the controller. However, further work is required before this information can be acted upon in a closed-loop manner. A control system has, however, been developed to allow control of the temperature across the powder bed and as a result, the material microstructure can be influenced.

## 5.2. Directed Energy Deposition

The DED processes are similar to the PBF processing in some ways; much of the pre-processing work is common across all processes, such as slicing of the model into layers before being built into a physical part. A key difference is that for DED processes, the focused energy beam is not melting a powder onto a bed, but rather delivering a powder [69] or wire into a molten pool on the substrate surface [70,71]. Co-ordinated movement of the energy source and material injection mechanism completes the layers in order to create a part. As such, no post-process separation of the part from the powder bed is necessary. Further information about the process, commonly occurring material discontinuities and in-situ methods trialled so far, is given below.

### 5.2.1. Powder-DED

The powder-DED process was patented in 1996 by Jeantette et al. for the Sandia Corporation [72]. Atwood et al. (1998) have reported that the LENS™ process can produce parts with a dimensional accuracy of 0.05 mm in lateral directions and even better dimensional accuracy in the vertical direction, depending on layer height [73]. This powder-

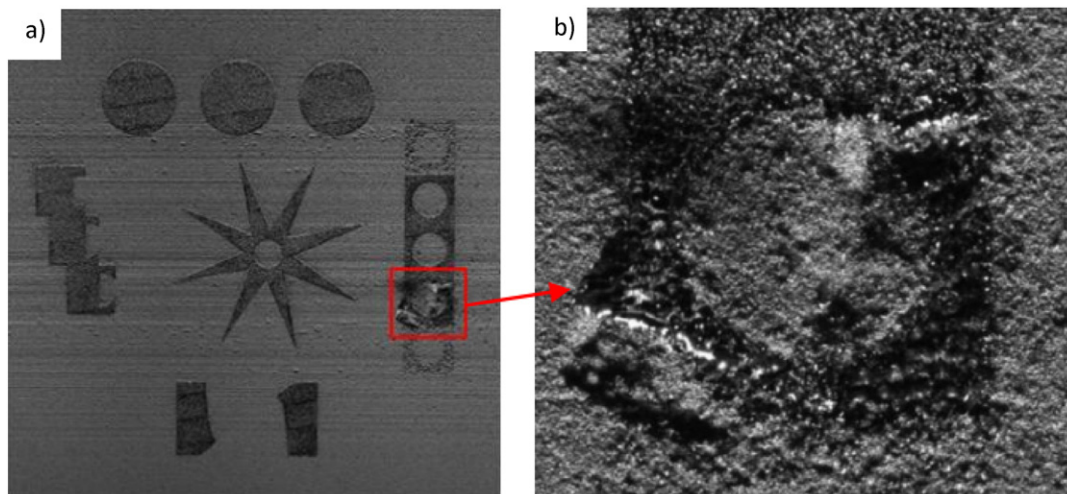
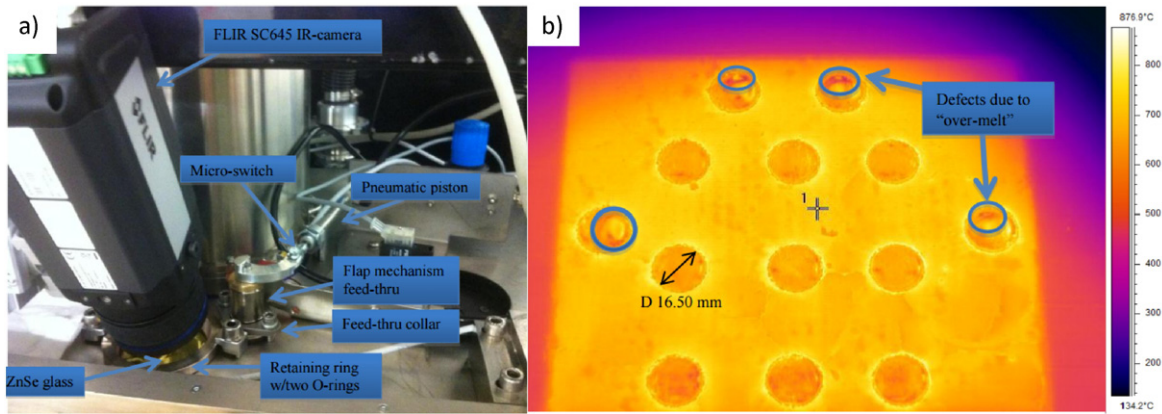


Fig. 7. Image taken using described high resolution imaging system (left) enlarged to show area of curling (right) by Kleszczynski et al. [62].





**Fig. 8.** (a) Showing Arcam A2 build chamber with new component location and IR-camera and (b) an image taken using IR camera with material discontinuities highlighted by Rodriguez et al. [66].

DED process has applications for complex 3D shapes as well as in-service repair operations with high strength and high ductility [74]. Materials research for LENS™ has shown that high quality parts can be produced with low-alloy steels, stainless steels [75], nickel-based alloys [76] and titanium alloys [77]. Powder-DED processes, such as LENS™, are investigated in particular due to its wide application range. Vision systems are particularly suitable because of ease of access, automation and reliability.

Predominantly, in-situ inspection methods have been implemented to improve the geometrical accuracy of components built by powder-DED. Two common material discontinuities that limit the material quality are porosity and cracks. There are two forms of porosity: trapped gas and porosity caused by lack of fusion between layers – this is likely caused by insufficient energy density in the melt pool. Gas porosity is thought to occur due to high powder flow rate, causing shielding gas to become entrapped within the melt pool. Cracking is likely caused due to differences in material thermal expansion coefficients or because of powder contamination [78]. Process windows for material systems have been developed and recent advances in the field allow multiple materials to be delivered [79]. The use of multiple materials adds a further complication to identifying discontinuities where material constituents have vastly different mechanical and optical properties.

Wang et al. investigated the thermal behaviour of stainless steel 410 during powder-DED processing, both numerically and experimentally, using pyrometry and a vision based system [80]. Data was captured by a two-wavelength pyrometer, positioned outside a LENS 850 machine and directed through the thin film in the viewport, as shown in Fig. 9. The Si-based digital CCD camera captured a field of view 22 mm × 25 mm, recording an image every 2 s. Bandwidths of 700 nm to 800 nm and 800 nm to 900 nm were selected. The pyrometer recorded in the temperature range of 1450 °C to 1860 °C. It was shown that a

near-infrared filter was needed to minimise the noise factors such as metallic vapour, a heated air zone above the molten pool and airborne metallic powder; laser radiation was also found to distort the images. The numerical analysis showed good capability for predicting melt pool size and temperature distribution. The thermal model was used to evaluate in-process measurements. Rather than for the purpose of implementing a closed-loop control system, this research was geared towards developing an improved understanding of the process.

Hua et al. have since shown that pyrometry data can be used to correlate melt pool size and layer thickness during powder-DED in such a way that this data can be used for closed-loop control [81]. In order to determine the effect of powder feed rates and laser power on melt pool uniformity, it was shown by Yu et al., through pyrometry measurements, that the solidification time of the melt pool can change drastically [82]. A similar approach has been taken by Medrano Téllez, who used pyrometry to control bead geometry (height and width) of wire-DED in a closed-loop fashion [83]. Pyrometry has also been used by Nassar et al. to aid in development of a closed-loop build strategy controller for a LENS™ system. The system collects temperature data which is used to select a location for the next deposition path, avoiding areas above a pre-set temperature threshold. The system results in more uniform material characteristics and properties although does increase build time by a third [84].

Griffiths et al. were amongst the first to investigate the use of IR imaging for in-situ measurement of powder-DED [85]. An IR camera was used to assess the relative temperatures seen when processing stainless steel 316 using the LENS™ process. A 320 × 244 pixel CCD array recording element with spectral range from 3.6 mm to 5 mm was used to take images of the melt pool, which were also compared with images taken using a high speed camera, and temperatures were obtained using standard pyrometry techniques. As emissivity data for powder-DED

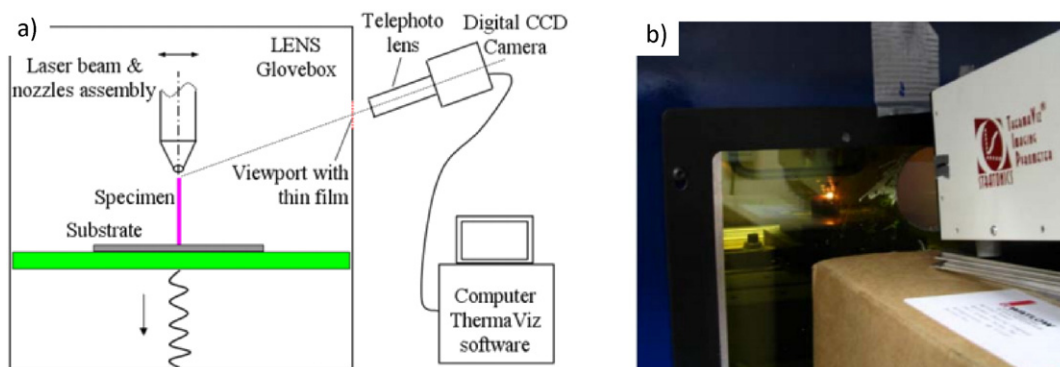


**Fig. 9.** (a) Schematic of digital CCD camera focussed through viewport for thermal behaviour analysis of SS410 and (b) photograph of set-up selected by Wang et al. [80].

manufactured components was not known, all temperatures calculated were relative. Output images show the melt pool and surrounding zones heated by conduction. A thermal profile was plotted relative to the maximum temperature seen at the weld pool. Hu and Kovacevic instead utilised a near-infrared (NIR) camera in combination with a powder delivery rate sensor for melt pool monitoring during powder DED processing [86]. A co-axial IR imaging camera with 800 frames/s framerate was used to take grey-scale images of the melt pool area with a  $128 \times 128$  pixel resolution. An appropriate filter was used to protect the camera from damage by the processing laser. A greater than 700 nm IR filter was also implemented to improve the image quality. A linked PC performed the image processing and control steps outlined in Fig. 10(a). Temperature distribution in the meltpool was assessed from the IR image (Fig. 10(b)) using grey level isotherms (Fig. 10(c)). A closed-loop control system was developed for heat input control, yielding improvements in geometrical part accuracy using real-time control, specifically for functionally graded components.

Karnati et al. have also investigated monitoring the temperature variation and build height during powder-DED LENS<sup>TM</sup> production [87]. Two closed-loop feedback systems were integrated to maintain the amount of energy per deposition and another to measure build height. A FLIR A615 IR camera with a resolution of  $640 \times 480$  pixels and a spectral range of  $8 \mu\text{m}$  to  $14 \mu\text{m}$  was used to thermally analyse the deposition of stainless steel 304. Power modulations were found to decay exponentially and stabilise around a range. Peaks were found to correlate with instances where the laser beam was at the extremes of the geometry. This stabilisation indicated that an optimum set of parameters can be developed for any material system and that, through control of the high temperature region, material properties can be tailored or homogenised. Following on from this, Barua et al. employed a Canon EOS 7D SLR camera for melt pool monitoring and discontinuity detection [78]. The camera system was mounted within the (unspecified) powder-DED machine, perpendicular to the deposition direction. The obtained images were analysed and the intensity of light radiating from the melt pool was used to determine the temperatures, once the optical system had been calibrated. Material discontinuities such as holes (0.32 mm diameter) and cracks (0.04 mm wide) were artificially created in testpieces that were then deposited on. It was found that the discontinuities could be observed with the camera setup and their locations could be identified, however, no sizing information could be delivered. Real-time processing of the images was not possible, due to a mismatch in the photograph capture frame rate (7 frames/s) and the interrogation software processing time per image (1 s). Changes in light intensity, rather than actual temperature change was monitored, thus temperature calibration was not needed. Tang and Landers have shown that stabilising melt pool temperature alone in order to produce uniform track morphology to be insufficient [88]. Melt pools of different

sizes can have the same temperature profile, hence further information regarding the thermal characteristics of the powder material and substrate materials need to be considered for full control.

Instead of using a pyrometry or IR-based inspection processes, Wang et al. have utilised acoustic emission testing to identify crack formation in powder-DED [89]. An acoustic sensor was placed at each end of the substrate being built on and the signals were recorded with an acoustic emission detection device. The position of the crack and time of generation were attained through post-processing of the data, so currently, this is not a real-time option. However, it was shown that increases in layer thickness leads to an increase in crack formation due to higher cooling rate and this method could have potential for closed-loop control.

The above studies have shown that the use of both pyrometry and IR cameras allows for in-situ monitoring of powder-DED processing. In some cases, monitoring methods have been linked with process inputs to allow for closed-loop control of the process; however, in order for simultaneous control of the melt pool temperature and track morphology, further a priori knowledge regarding the material and component is required.

### 5.2.2. Wire-DED

Although the wire-DED process differs from powder-DED processes in terms of material delivery, many of the same material discontinuities are found and as such, the same approaches to monitor the process in-situ can be used. For example, Zalameda et al. opted to use a NIR camera to ensure weld integrity during wire-DED processing [90]. The camera was mounted at  $60^\circ$  to the weld pool, in-line with the weld bead and was calibrated with a black body radiation source. The weld pool area was imaged successfully, allowing an improved weld to be produced. The transient section of the weld response curve was also used to analyse the weld, non-destructively. Although further measurements were required, this study showed the potential for dual use of an IR imaging camera for both closed-loop control and inspection.

Conversely, Liu et al. used an optical emission spectrometer to detect the emission signal of the plasma plume generated over the molten pool of Inconel 625 wire deposited using laser hot-wire welding [91]. A correlation between the results of spectroscopic analysis and the clad quality was determined for properties such as surface appearance, clad dilution, hardness and microstructure. In addition, a high speed CCD camera in combination with a green light laser was used to monitor the melt pool, at a rate of 250 frames/s. The set-up is shown in Fig. 11. It was found that plasma electron temperature (of the plasma that formed over the melt pool) could be used as an indicator of clad quality and stability of the process, as an increase in the standard deviation of the plasma electron temperature implied an instability, such as an arc or splatter. Similar works have been carried out for powder-DED

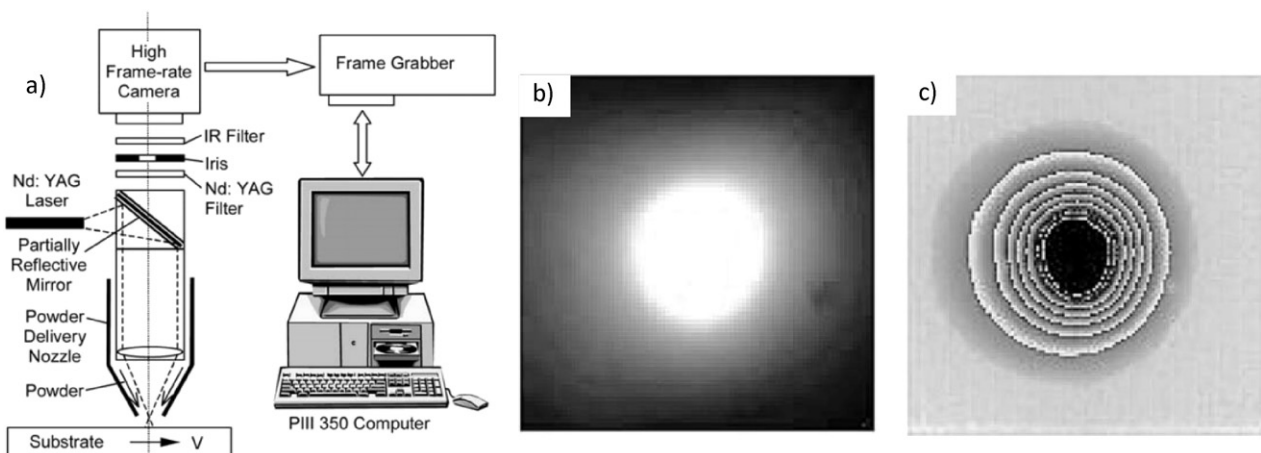


Fig. 10. (a) Schematic of equipment set-up, (b) IR image of meltpool and (c) grey level analysis conducted by Hu and Kovacevic [86].

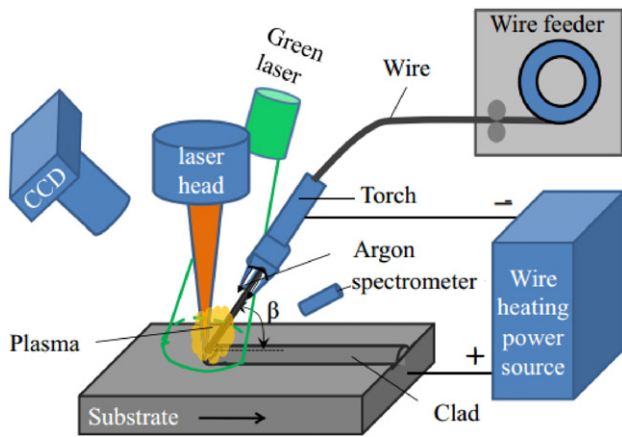


Fig. 11. Schematic diagram of experimental set-up for laser hot-wire deposition used by Liu et al. [91].

processes [92–94], with Nassar et al. suggesting that optical emission spectrometry is suitable for identifying lack of fusion defects [95].

An alternative approach to in-situ monitoring, utilising a 3D scanner for laser triangulation, set-up on a modified laser welding system processing Ti–6Al–4V, has been trialled by Heralić et al. [96]. The team have been able to show that the data that can be obtained is useful for the detection of in-process disturbances. In addition, a control algorithm was developed to incorporate the a priori 3D layer data and an iterative learning approach was employed to adjust layer heights, in order to avoid geometrical inaccuracies. This system was focused on geometrical data and the experimental set-up is shown in Fig. 12.

Again, it is predominantly optical or thermal systems that have been selected for in-situ inspection of components manufactured by both DED processes; more novel methods are yet to be trialled. It is clear that there is a drive towards in-line inspection and the studies have shown that closed-loop control for certain cases can be achieved. However, the research has been mainly focussing on in-process feedback in order to optimise build parameters and hence increasing the accuracy of the processes from a geometrical point of view. Material properties, microstructure and material discontinuities have rarely been investigated using these methods and instead, destructive evaluation is commonly employed.

### 5.3. Other potential NDT processes

Building on the more novel methods that have been trialled for in-situ inspection of the DED process, the following processes have been identified as having potential for in-situ inspection of PBF and DED processes, but are yet to have been integrated on a processing machine.

Instead, neutron diffraction, laser ultrasonic testing and X-ray backscatter technology have been trialled on AM testpieces, post-build.

Watkins et al. highlight the capability of neutron diffraction to non-destructively determine residual strains and stresses for AM components manufactured by wire-DED and laser-PBF in particular [97]. They compare XCT with neutron computed tomography, pointing out the superior penetration depth of neutrons over X-rays. Both methods use diffraction theory to describe scattering from single crystals, powders or polycrystalline solids, but X-ray scattering occurs within a few micrometres or millimetres, whereas neutrons can penetrate to several centimetres. Neutron radiographs are produced using a LiF/ZnS scintillator, converting neutrons into light which can then be detected by a CCD camera. At present, work is limited to be carried out at larger national and international synchrotron facilities, although portable neutron sources do exist. General information regarding neutron imaging in the wider sense can be found elsewhere [98–101].

Laser ultrasonics (LU) is another technique which is being developed for use on AM components. LU uses lasers to both generate and detect ultrasonic waves and can be used to detect material discontinuities, for materials characterisation and to determine material thickness. A pulsed laser is used to generate an ultrasonic wave and a continuous-wave laser interferometer detects the small surface displacement when the wave arrives at the detection point (Fig. 13); surface acoustic waves (Rayleigh waves), longitudinal waves (p waves) and shear waves (s waves) can be analysed. LU is non-contact and can be used on curved or difficult to access areas making it suitable for application to AM [102].

Edwards et al. have investigated the transmission and enhancement of laser generated surface waves with surface breaking angled cracks, wedge-shaped samples and branched cracks [103]. A pulsed Nd:YAG laser with 1064 nm wavelength and 10 ns pulse duration was focussed into a line scanning laser line of 6 mm by 300  $\mu$ m. A filter was applied, limiting the generation to a Rayleigh wave with central frequency of 1.67 MHz in the thermoelastic regime. An IOS two-wave mixer interferometer was used as a detector. The experiment was also modelled using PZFlex FEM software. Experimental results showed that knowledge of the internal geometry of the crack is required in order to obtain an accurate depth profile and that branching near the surface makes a measurement more complex. Klein and Sears also used a pulsed Nd:YAG laser at 1064 nm wavelength, however, in this instance in the ablation regime. A Lasson AIR-532-TWM laser ultrasonic receiver was used – operating at 532 nm. The focussed area was 100  $\mu$ m to 300  $\mu$ m and the laser pulse energy in the range of 10 mJ to 30 mJ. Simulated cracks in the un-polished powder-DED sample were detected using a computationally efficient processing approach which can now be expanded upon to develop an in-line, real-time system [102]. Klein also has a related patent entitled “Laser-ultrasonic detection of subsurface defects in processed metals”. The claims cover detection for voids, pores, bondlines, disbands and cracks in laser clad and friction stir processed metals. Specific wavelength generators and detectors are covered, along with various analysis methods such as wavelet analysis [104].

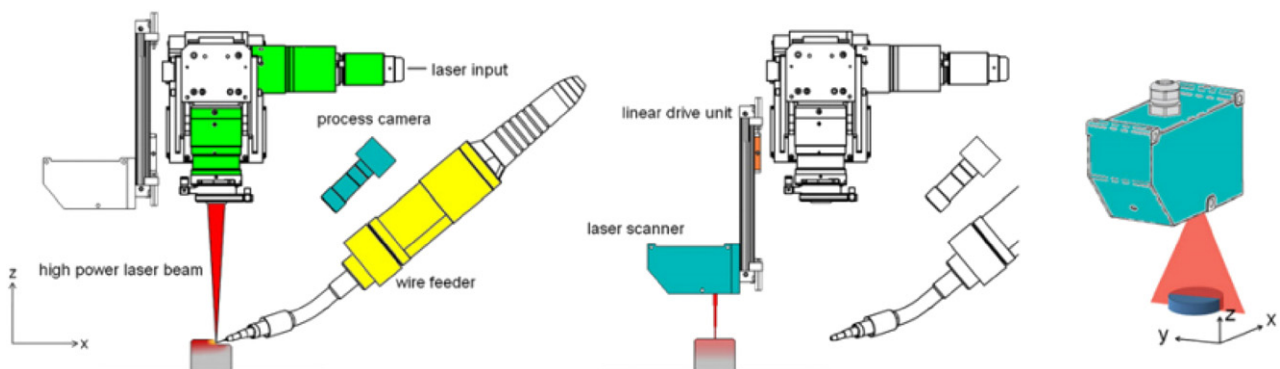


Fig. 12. Experimental set-up of Laser scanning and CMOS devices on a modified laser welding system selected by Heralić et al. [96].



Clark et al. have performed a similar LU experiment on a range of samples produced by laser-PBF, using a Q-switched mode-locked Nd:YAG laser with wavelength 1064 nm. A 12.2 ns pulse duration resulted in a high frequency Rayleigh wave of 82 MHz which is very sensitive to optical scattering. Consequently, the titanium and nickel based alloy samples were polished to optimise their acoustic and optical reflection properties. The density of the samples was evaluated and the technique was shown to have promise [105]. Clark et al. had previously had a European patent granted covering the integration of non-destructively analysing the properties of a layer with a laser-generated non-contact ultrasonic wave pattern, detecting the wave and analysing it with layer-based deposition manufacture [106]. Eddy current analysis and closed-loop control of the speed, movement or focus of a laser beam are also included. As a continuation of this work, a non-destructive laser ultrasound method named spatially resolved acoustic spectroscopy (SRAS) has been shown, by Li et al., to give information of crystallographic orientation of metals (here: Al and Inconel 617) [107]. Specifically, the SRAS detection method has been used for rapid imaging of material microstructure and grain orientation on polished Ti64 surfaces with a knife edge detector (a two photodiode differential signal analysis sensor) [108]. Due to the surface acoustic waves propagating through the bulk of the material, it is possible to detect subsurface discontinuities by reflections against grain boundaries and discontinuities in the bulk of the material. By increasing acquisition speed and the pulsed laser frequency, the processing time has been reduced by a factor of 80. Since AM samples are rougher than the surface required for measurement using the knife edge detector, the next generation of the SRAS tool incorporates rough surface measurement capabilities with the speckle knife edge detector [109].

Ultrasonic testing can be effective for detecting flaws, thickness, grain size, density/porosity and mechanical properties of materials, but its use is limited to in-situ inspection of ultrasonic consolidation (UC) as contact ultrasound cannot function above 500 K [110]. The inspection system was integrated into the x-axis motor of a Fabrionics machine. A precision linear motor was used for motion in the y-axis and a stepper motor used for focusing in the z-axis. Isopropyl alcohol was used as a contact medium for the transducer as it is cheap and does not have any detrimental effect on the metal being processed. The contact medium evaporated after measurements were taken. Although the method was found to give adequate results, the measurement system is highly sensitive to surface finish and grain noise. An alternate method of utilising ultrasonic inspection has been developed by Reider et al. who have integrated an ultrasonic probe into the base-plate of a laser-PBF machine [111]. The system is able to record ultrasonic signals with a temporal resolution of 4 ns, taking 1000 scans per second. Recording data over an 8-h build cycle does result in many gigabytes of data which is currently stored and processed off-line.

X-ray backscatter technology (XBT) is suited to use for inspecting AM parts as it is not susceptible to surface roughness. Large structures can be easily tested due to the X-ray source and detector being

positioned on the same side of an object; real time imaging allows recursive scanning. Georgeson et al. presented an overview of possible applications of XBT to the aerospace sector generally, particularly in corrosion detection, foreign object damage detection, fluid intrusion and in finding cracks and voids [112]. Highlighted challenges to adopting XBT include developing standards and procedures, the large equipment required for high scanning speeds and the limited availability of tailored X-ray sources. More specifically to AM, the capability of XBT to detect cracks below a deposit has been investigated by Naito et al. [113]. Previously, inspection times for detecting a microcrack have been unacceptably long; however, using uncollimated X-ray irradiation, a larger surface area can be inspected at any one time. The X-ray irradiation equipment comprised a pinhole X-ray image intensifier (X-ray II Toshiba E5889BE-P1K) connected to a Bitran BS-42, 40 megapixel CCD camera and a small, highly intensive X-ray generator (tube voltage 80 kV and tube current of 4 mA), which was positioned 300 mm from the pinhole at an angle of 10° to 30°. Two types of 0.1 mm pinholes were trialled – one with a single conical hole and a second with two back-to-back conical holes (hourglass). The intensity distribution of (back)scattered X-rays from the component was measured. Cracks showed up as dark areas as they hardly scatter the X-rays. Artificial slits with greater than 0.05 mm width were detected by the back-to-back pinholes, although an increased intensity could reduce this to 0.025 mm. Testpieces covered with a stainless steel plate were manufactured. The crack-detectable deposit thickness was 0.7 mm when the crack was 0.025 mm width and 0.5 mm depth – the deposit is a metal oxide deposit of 1.2 g cm<sup>-3</sup>. An artificial stress corrosion crack below an artificial deposit of iron oxide in a curved testpiece was also detected.

Although these more novel NDT methods have potential for in-situ inspection of AM processes, the increased complexity of integration within the processing environment suggests that camera or thermal based methods will likely be favoured. However, the simpler methods are limited to inspection of the top processing surface only. The more novel methods detailed in this section, although trickier to integrate, facilitate greater inspection penetration into the material and have the potential to identify material discontinuities, and assess material characteristics such as microstructure.

## 6. The underpinning metrology challenge: future direction

Vision-based and thermal metrology solutions go some way to addressing the quality control issues with AM, but what is needed specifically, is the ability to characterise 3D structures over relatively large areas (up to several centimetres squared) to very high spatial resolution. Furthermore, such metrology solutions need to be fast and compatible with the production environment.

The AM metrology task is increasingly limited by the fundamentals of optical interrogation of the surface, such as: the compromise between spatial resolution and field of view; the loss of effective spatial

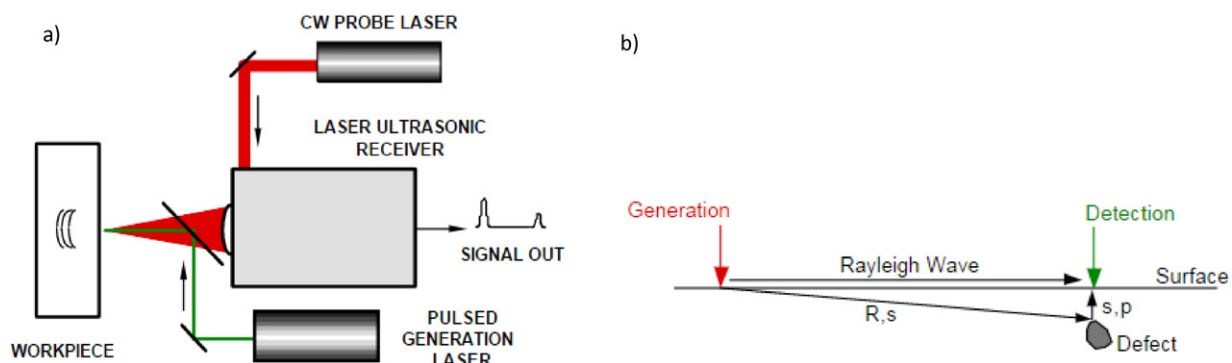


Fig. 13. (a) Schematic of laser-based ultrasound and (b) inspection geometry using Rayleigh (surface) waves implemented by Klein and Sears [102].

resolution due to motion blur; or the dynamic range of optical properties across the inspected region. Such limits imply that faster “brute-force” measurement of the whole surface presents significant data management and analysis challenges.

In order to overcome the in-process metrology challenge, it is essential to exploit a priori knowledge about the production task, and the nature and functional significance of relevant material discontinuities to dramatically simplify the measurement task. Development of existing measurement techniques to simplify integration, hybridisation and increase environmental tolerance will also help. Appropriate preparation should produce opportunities to simplify the measurement task and increase throughput. In addition to identification of material discontinuities, it is prudent to consider how product function and price vary with the severity of the discontinuity, so that the economics of detection can be quantitatively optimised. If discontinuities across the surface of interest are correlated somehow and have a cumulative effect, representative areas may yield enough information for real-time decision-making. Alternatively, if a single local discontinuity can have a large functional effect, 100% inspection might be obligatory, but only in pre-defined areas such as the track followed by the energy beam.

Smarter measurement planning methods then follow. One potential solution to the AM metrology challenge is the use of hybrid instrumentation, i.e. to detect areas of interest with a relatively low resolution sensor (for example, camera-based sensors), then to “home-in” on the areas of interest using a localised, high resolution sensor (see for example, [114,115]). Data fusion techniques can then be used to combine the data from the different sensors [116,117]. In some scenarios the low resolution sensor could use approaches that detect light scattered from points of interest, such as scratches, therefore, allowing high resolution detection without the need for imaging. The low-resolution sensor might also have a functional basis. Development of techniques to address the metrology challenge requires advances in a number of mathematical areas. Where two or more sensors are used with different lateral resolutions, data fusion techniques are required to combine the data and to match the co-ordinate systems of the sensors [117]. To reduce scanning times and make full use of all the available information, intelligent sampling techniques will need to be utilised [118]. One relatively promising newcomer to this field is compressed sensing [119], although it has not been demonstrated on AM-type applications yet (to the knowledge of the authors). Lastly, methods need to be developed for handling the potentially very large datasets that will be produced when measuring to high resolution over relatively large areas, such as the method demonstrated by Kriczky et al. [120].

While the AM metrology challenge cannot be solved by sensor development alone, such development is important. Significant advances have been made in the field of surface topography measurement over the last three decades, from the development of optical instrumentation, which is now a fully-fledged rival to contacting techniques, to the development of specification standards for areal topography. However, there are two distinct classes of instrument: (a) those that measure over large areas (metres squared) with tens to hundreds of micrometres spatial resolution (for example, fringe projection, photogrammetry and Moiré interferometry) [121], and (b) those that measure over small areas (up to a few millimetres squared) with spatial resolutions of the order of a micrometre (for example, coherence scanning interferometry (CSI), confocal microscopy and focus variation microscopy (FVM)) [122]. Essentially, the former class is camera-limited, and the latter is objective-limited. There have been several attempts to try and combine the two classes (see for example [123]), but more progress is required before such hybrids can be used in AM manufacturing.

## 7. Conclusions

From the literature reviewed in this paper, a number of concluding remarks can be made. Firstly, it is clear that there is an industry pull for in-situ inspection and closed-loop control techniques for AM and

as a result, many global institutions are actively conducting research in this area. Many of the systems that have been developed to date allow for monitoring of AM processes simply in order to better understand the processes, rather than for in-process identification of material discontinuities. Visual, camera-based methods have been used to identify processing errors for PBF, such as powder bed condition and geometrical accuracy. For DED, closed-loop feedback has been achieved when monitoring build height using vision-based systems. Pyrometry and use of IR cameras has allowed for closed-loop control of PBF in order to maintain a constant temperature gradient across the build area although existing patents and licensing agreements, along with the harsh processing environment, limit the integration of monitoring equipment within the AM machines and as a result, externally mounted solutions have been favoured.

In-situ methods that have been implemented to date largely only yield information about the component surface; other more advanced NDT techniques that can inspect sub-surface have been tested ex-situ, but are yet to be integrated. Real-time identification and closed-loop control of parameters, in order to minimise material discontinuities, is limited by poor spatial resolution, limited fields of view, high temporal load and by the large amounts of data to be handled. For effective closed-loop control, a priori knowledge of the part and build process is required. Development of new sensors which allow for inspection with a resolution consistent with commonly occurring material discontinuities is needed.

## Acknowledgements

This paper incorporates work carried out by the lead author at Manufacturing Technology Centre under core research project A10697. The authors would also like to acknowledge the UK Research Centre in Non-Destructive Evaluation (RCNDE) (EPSRC grant EP/L022125/1), ‘In-situ monitoring of component integrity during additive manufacturing using optical coherence tomography’ (EPSRC grant EP/L01713X/1) and ‘Metrology for precision and additive manufacturing’ (EPSRC grant EP/M008983/1).

## References

- [1] T.T. Wohlers, Wohlers Report, Wohlers Associates, 2015 2015.
- [2] K.F. Martin, A review by discussion of condition monitoring and fault diagnosis in machine tools, *Int. J. Mach. Tools Manuf.* 34 (4) (1994) 527–551.
- [3] S. Adamczak, J. Bochnia, B. Kaczmarek, An analysis of tensile test results to assess the innovation risk for an additive manufacturing technology, *Metrol. Meas. Syst.* 22 (1) (2015) 127–138.
- [4] J.P. Kruth, Material increment manufacturing by rapid prototyping techniques, *CIRP Ann. Manuf. Technol.* 40 (2) (1991) 603–614.
- [5] J.P. Kruth, G. Levy, F. Klocke, T.H.C. Childs, Consolidation phenomena in laser and powder-bed based layered manufacturing, *CIRP Ann. Manuf. Technol.* 56 (2) (2007) 730–759.
- [6] J. Giannatsis, V. Dedoussis, Additive fabrication technologies applied to medicine and health care: a review, *Int. J. Adv. Manuf. Technol.* 40 (1–2) (2009) 116–127 English.
- [7] J. Ciurana, Designing, prototyping and manufacturing medical devices: an overview, *Int. J. Comput. Integr. Manuf.* 27 (10) (2014) 901–918.
- [8] A. Uriondo, M. Esperon-Miguez, S. Perinpanayagam, The present and future of additive manufacturing in the aerospace sector: a review of important aspects, *Proc. Inst. Mech. Eng. Part G: J. Aerosp. Eng.* 229 (11) (2015) 2132–2147.
- [9] G.N. Levy, R. Schindel, J.P. Kruth, Rapid manufacturing and rapid tooling with layer manufacturing (LM) technologies, state of the art and future perspectives, *CIRP Ann. Manuf. Technol.* 52 (2) (2003) 589–609.
- [10] W.E. Frazier, Metal additive manufacturing: a review, *J. Mater. Eng. Perform.* 23 (6) (2014) 1917–1928 (2014/06/01, English).
- [11] T.B. Sercombe, X. Xu, V.J. Challis, R. Green, S. Yue, Z. Zhang, et al., Failure modes in high strength and stiffness to weight scaffolds produced by Selective Laser Melting, *Mater. Des.* 67 (2015) 501–508.
- [12] D. Cooper, J. Thornby, N. Blundell, R. Henrys, M.A. Williams, G. Gibbons, Design and manufacture of high performance hollow engine valves by Additive Layer Manufacturing, *Mater. Des.* 69 (2015) 44–55.
- [13] C. Qiu, G.A. Ravi, M.M. Attallah, Microstructural control during direct laser deposition of a  $\beta$ -titanium alloy, *Mater. Des.* 81 (2015) 21–30.
- [14] G. Tapia, A. Elwany, A review on process monitoring and control in metal-based additive manufacturing, *J. Manuf. Sci. Eng.* 136 (6) (2014) 60801–60811.

- [15] ASTM Standard, Standard terminology for additive manufacturing technologies, ASTM Standard F2792-12a, ASTM International, West Conshohocken, PA, 2012.
- [16] AM Special Interest Group, in: T.S. Board (Ed.), Shaping our national competency in additive manufacturing, Online: UK Government, 2012.
- [17] I. Gibson, D.W. Rosen, B. Stucker, Additive Manufacturing Technologies: Rapid Prototyping to Direct Digital Manufacturing, Springer, 2009.
- [18] Energetics Incorporated, Measurement Science Roadmap for Metal-Based Additive Manufacturing, National Institute of Standards and Technology, Maryland, US, 2013.
- [19] AM Steering Group UK, Steering Group, 2015 [6th October]. Available from: <http://www.amnationalstrategy.uk/steering-group/>.
- [20] AM Steering Group UK, Positioning paper: the case for additive manufacturing, 2015 6th October 2015. Available from: <http://www.amnationalstrategy.uk/wp-content/uploads/2015/05/AM-Strategy-Positioning-Paper.pdf>.
- [21] ISO/TC 261, Additive manufacturing, 2011 [cited 2015 4th November]. Available from: [http://www.iso.org/iso/home/standards\\_development/list\\_of\\_iso\\_technical\\_committees/iso\\_technical\\_committee.htm?commid=629086](http://www.iso.org/iso/home/standards_development/list_of_iso_technical_committees/iso_technical_committee.htm?commid=629086).
- [22] BS ISO/ASTM International, Standard terminology for additive manufacturing: Coordinate systems and test methodologies. ISO/ASTM52921 - 13, ISO, Geneva, Switzerland, 2013.
- [23] BS ISO/ASTM International, Standard specification for additive manufacturing file format (AMF) Version 1.1 ISO/ASTM52915 - 13, ISO, Geneva, Switzerland, 2013.
- [24] BS ISO, Additive manufacturing. General principles. Part 4: overview of data processing ISO 17296-4:2014, ISO, Geneva, Switzerland, 2014.
- [25] BS ISO, Additive manufacturing. General principles. Part 3: main characteristics and corresponding test methods ISO 17296-3:2014, ISO, Geneva, Switzerland, 2014.
- [26] BS ISO, Additive manufacturing. General principles. Part 2: overview of process categories and feedstock. ISO 17296-2:2015, ISO, Geneva, Switzerland, 2015.
- [27] J.-P. Kruth, P. Mercelis, J.V. Vaerenbergh, L. Froyen, M. Rombouts, Binding mechanisms in selective laser sintering and selective laser melting, *Rapid Prototyp. J.* 11 (1) (2005) 26–36.
- [28] J. Schwerdtfeger, R.F. Singer, C. Körner, In situ flaw detection by IR-imaging during electron beam melting, *Rapid Prototyp. J.* 18 (4) (2012) 259–263.
- [29] L.E. Murr, S.M. Gaytan, D.A. Ramirez, E. Martinez, J. Hernandez, K.N. Amato, et al., Metal fabrication by additive manufacturing using laser and electron beam melting technologies, *J. Mater. Sci. Technol.* 28 (1) (2012) 1–14.
- [30] E.O. Olakanmi, R.F. Cochrane, K.W. Dalgarno, A review on selective laser sintering/melting (SLS/SLM) of aluminium alloy powders: processing, microstructure, and properties, *Prog. Mater. Sci.* 74 (10) (2015) 401–477.
- [31] X. Gong, T. Anderson, K. Chou, Review on powder-based electron beam additive manufacturing technology, *Manuf. Rev.* 1 (1) (2014) 12–24.
- [32] M. Van Elsen, Complexity of Selective Laser Melting: A New Optimisation Approach [EngD], Katholieke Universiteit Leuven, Belgium, 2007.
- [33] L. Thijs, F. Verhaeghe, T. Craeghs, J.V. Humbeek, J.-P. Kruth, A study of the microstructural evolution during selective laser melting of Ti–6Al–4V, *Acta Mater.* 58 (9) (2010) 3303–3312.
- [34] H. Attar, M. Calin, L.C. Zhang, S. Scudino, J. Eckert, Manufacture by selective laser melting and mechanical behavior of commercially pure titanium, *Mater. Sci. Eng. A* 593 (1) (2014) 170–177.
- [35] S. Clijsters, T. Craeghs, S. Buls, K. Kempen, J.P. Kruth, In situ quality control of the selective laser melting process using a high-speed, real-time melt pool monitoring system, *Int. J. Adv. Manuf. Technol.* 75 (5) (2014) 1089–1101 (English).
- [36] S. Tammas-Williams, H. Zhao, F. Léonard, F. Derguti, I. Todd, P.B. Prangnell, XCT analysis of the influence of melt strategies on defect population in Ti–6Al–4V components manufactured by selective electron beam melting, *Mater. Charact.* 102 (4) (2015) 47–61.
- [37] A.A. Antonyasamy, J. Meyer, P.B. Prangnell, Effect of build geometry on the  $\beta$ -grain structure and texture in additive manufacture of Ti6Al4V by selective electron beam melting, *Mater. Charact.* 84 (10) (2013) 153–168.
- [38] R. Li, J. Liu, Y. Shi, L. Wang, W. Jiang, Balling behavior of stainless steel and nickel powder during selective laser melting process, *Int. J. Adv. Manuf. Technol.* 59 (9–12) (2012) 1025–1035 English.
- [39] D. Gu, Y. Shen, Balling phenomena in direct laser sintering of stainless steel powder: metallurgical mechanisms and control methods, *Mater. Des.* 30 (8) (2009) 2903–2910.
- [40] P. Mercelis, J.-P. Kruth, Residual stresses in selective laser sintering and selective laser melting, *Rapid Prototyp. J.* 12 (5) (2006).
- [41] S.L. Campanelli, N. Contuzzi, A. Angelastro, A.D. Ludovico, in: M. Joo Er (Ed.), New trends in technologies: devices, computer, communication and industrial systems, Online: Sciyo, 2010 (454 p).
- [42] W. Shifeng, L. Shuai, W. Qingsong, C. Yan, Z. Sheng, S. Yusheng, Effect of molten pool boundaries on the mechanical properties of selective laser melting parts, *J. Mater. Process. Technol.* 214 (11) (2014) 2660–2667.
- [43] K.A. Mumtaz, P. Erasenthiran, N. Hopkinson, High density selective laser melting of Waspaloy®, *J. Mater. Process. Technol.* 195 (1–3) (2008) 77–87.
- [44] E. Yasa, J. Deckers, J.P. Kruth, The investigation of the influence of laser re-melting on density, surface quality and microstructure of selective laser melting parts, *Rapid Prototyp. J.* 17 (5) (2011) 312–327.
- [45] D. Gu, Y. Shen, Processing conditions and microstructural features of porous 316L stainless steel components by DMLS, *Appl. Surf. Sci.* 255 (5, Part 1) (2008) 1880–1887.
- [46] H.J. Niu, I.T.H. Chang, Instability of scan tracks of selective laser sintering of high speed steel powder, *Scr. Mater.* 41 (11) (1999) 1229–1234.
- [47] J.P. Kruth, L. Froyen, J. Van Vaerenbergh, P. Mercelis, M. Rombouts, B. Lauwers, Selective laser melting of iron-based powder, *J. Mater. Process. Technol.* 149 (1–3) (2004) 616–622.
- [48] M. Zaeh, G. Branner, Investigations on residual stresses and deformations in selective laser melting, *Prod. Eng. Res. Devel.* 4 (1) (2010) 35–45.
- [49] T. Purtonen, A. Kalliosaari, A. Salminen, Monitoring and adaptive control of laser processes, *Phys. Procedia* 56 (1) (2014) 1218–1231.
- [50] S. Berumen, F. Bechmann, S. Lindner, J.-P. Kruth, T. Craeghs, Quality control of laser- and powder bed-based Additive Manufacturing (AM) technologies, *Phys. Procedia* 5 (Part B) (2010) 617–622.
- [51] F. Herzog, F. Bechmann, S. Berumen, J.P. Kruth, T. Craeghs, Inventors Method for Producing a Three-Dimensional Component Patent WO1996008749 A3, 2013 (Aug 23, 1995).
- [52] T. Craeghs, S. Clijsters, J.P. Kruth, F. Bechmann, M.C. Ebert, Detection of process failures in layerwise laser melting with optical process monitoring, *Phys. Procedia* 39 (1) (2012) 753–759.
- [53] T. Furumoto, M.R. Alkahari, T. Ueda, M.S.A. Aziz, A. Hosokawa, Monitoring of laser consolidation process of metal powder with high speed video camera, *Phys. Procedia* 39 (1) (2012) 760–766.
- [54] T. Furumoto, T. Ueda, M.R. Alkahari, A. Hosokawa, Investigation of laser consolidation process for metal powder by two-color pyrometer and high-speed video camera, *CIRP Ann. Manuf. Technol.* 62 (1) (2013) 223–226 (PubMed PMID: WOS: 000322558000056).
- [55] T. Furumoto, T. Ueda, N. Kobayashi, A. Yassin, A. Hosokawa, S. Abe, Study on laser consolidation of metal powder with Yb:fiber laser—evaluation of line consolidation structure, *J. Mater. Process. Technol.* 209 (18–19) (2009) 5973–5980.
- [56] M. Pavlov, M. Doubenskaia, I. Smurov, Pyrometric analysis of thermal processes in SLM technology, *Phys. Procedia* 5 (Part B) (2010) 523–531.
- [57] M. Doubenskaia, M. Pavlov, Y. Chivel, Optical system for on-line monitoring and temperature control in selective laser melting technology, *Key Eng. Mater.* 437 (1) (2010) 458–461.
- [58] M. Islam, T. Purtonen, H. Piili, A. Salminen, O. Nyhrlä, Temperature profile and imaging analysis of laser additive manufacturing of stainless steel, *Phys. Procedia* 41 (1) (2013) 835–842.
- [59] H. Krauss, C. Eschey, M.F. Zaeh, Thermography for monitoring the selective laser melting process, 23rd International Solid Freeform Fabrication Symposium; Austin, TX, 2012.
- [60] T. Craeghs, S. Clijsters, E. Yasa, J.-P. Kruth, Online quality control of selective laser melting, 22nd International Solid Freeform Fabrication Symposium; Austin, TX, 2011.
- [61] P. Lott, H. Schleifenbaum, W. Meiners, K. Wissenbach, C. Hinke, J. Bültmann, Design of an optical system for the in situ process monitoring of selective laser melting (SLM), *Phys. Procedia* 12 (Part A) (2011) 683–690.
- [62] Error detection in laser beam melting systems by high resolution imaging, in: S. Kleszczynski, J. zur Jacobsmühlen, J. Sehr, G. Witt (Eds.), 23rd International Solid Freeform Fabrication Symposium; Austin, TX, 2012.
- [63] J. zur Jacobsmühlen, S. Kleszczynski, G. Witt, D. Merhof, Elevated region area measurement for quantitative analysis of laser beam melting process stability, 26th International Solid Freeform Fabrication Symposium; Austin, TX, 2015.
- [64] Thermographic in-situ process monitoring of the electron-beam melting technology used in additive manufacturing, in: R.B. Dinwiddie, R.R. Dehoff, P.D. Lloyd, L.E. Lowe, J.B. Ulrich (Eds.), SPIE Proceedings, 8705, 2013.
- [65] S. Price, J. Lydon, K. Cooper, K. Chou, Experimental temperature analysis of powder-based electron beam additive manufacturing, 24th International Solid Freeform Fabrication Symposium; Austin, TX, 2013.
- [66] E. Rodriguez, F. Medina, D. Espalin, C. Terrazas, D. Muse, C. Henry, et al., Integration of a thermal imaging feedback control system in electron beam melting, 23rd International Solid Freeform Fabrication Symposium; Austin, TX, 2012.
- [67] J. Mireles, C. Terrazas, F. Medina, R. Wicker, Automatic feedback control in electron beam melting using infrared thermography, 24th International Solid Freeform Fabrication Symposium; Austin, TX, 2013.
- [68] J. Mireles, C. Terrazas, S.M. Gaytan, D.A. Roberson, R.B. Wicker, Closed-loop automatic feedback control in electron beam melting, *Int. J. Adv. Manuf. Technol.* 78 (5) (2015) 1193–1199 English.
- [69] L. Costa, R. Vilar, Laser powder deposition, *Rapid Prototyp. J.* 15 (4) (2009) 264–279.
- [70] B.N. Turner, R. Strong, S.A. Gold, A review of melt extrusion additive manufacturing processes: I. Process design and modeling, *Rapid Prototyp. J.* 20 (3) (2014) 192–204.
- [71] B.N. Turner, S.A. Gold, A review of melt extrusion additive manufacturing processes: II. Materials, dimensional accuracy, and surface roughness, *Rapid Prototyp. J.* 21 (3) (2015) 250–261.
- [72] F.P. Jeantette, D.M. Keicher, J.A. Romero, L.P. Schanwald, Inventors Method and System for Producing Complex-Shape Objects, 2000.
- [73] C. Atwood, M. Ens, D. Greene, M. Griffith, L. Harwell, D. Reckaway, et al., Laser engineered net shaping (LENS(TM)): a tool for direct fabrication of metal parts, 17th International Congress on Applications of Lasers and Electro-Optics; Orlando, FL, 1998.
- [74] G. Bi, A. Gasser, K. Wissenbach, A. Drenker, R. Poprawe, Characterization of the process control for the direct laser metallic powder deposition, *Surf. Coat. Technol.* 201 (6) (2006) 2676–2683.
- [75] L. Wang, S.D. Felicelli, P. Pratt, Residual stresses in LENS-deposited AISI 410 stainless steel plates, *Mater. Sci. Eng. A* 496 (1–2) (2008) 234–241.
- [76] W. Liu, J.N. Dupont, In-situ reactive processing of nickel aluminides by laser-engineered net shaping, *Metall. Mater. Trans. A* 34 (11) (2003) 2633–2641 English.
- [77] S.M. Kelly, S.L. Kampe, Microstructural evolution in laser-deposited multilayer Ti–6Al–4V builds: part I. Microstructural characterization, *Metall. Mater. Trans. A* 35 (6) (2004) 1861–1867 English.



- [78] S. Barua, F. Liou, J. Newkirk, T. Sparks, Vision-based defect detection in laser metal deposition process, *Rapid Prototyp. J.* 20 (1) (2014) 77–85.
- [79] T.E. Abioye, Laser Deposition of Inconel 625/Tungsten Carbide Composite Coatings by Powder and Wire Feedstock: University of Nottingham, 2014.
- [80] Thermal modeling and experimental validation in the LENS™ process, in: L. Wang, S. Felicelli, J. Craig (Eds.), 18th International Solid Freeform Fabrication Symposium; Austin, TX, 2007.
- [81] T. Hua, C. Jing, L. Xin, Z. Fengying, H. Weidong, Research on molten pool temperature in the process of laser rapid forming, *J. Mater. Process. Technol.* 198 (1–3) (2008) 454–462.
- [82] J. Yu, X. Lin, J. Wang, J. Chen, W. Huang, Mechanics and energy analysis on molten pool spreading during laser solid forming, *Appl. Surf. Sci.* 256 (14) (2010) 4612–4620.
- [83] A.G. Medrano Téllez, Fibre Laser Metal Deposition with Wire: Parameters Study and Temperature Control, University Of Nottingham, 2010.
- [84] A.R. Nassar, J.S. Keist, E.W. Reutzel, T.J. Spurgeon, Intra-layer closed-loop control of build plan during directed energy additive manufacturing of Ti–6Al–4V, *Addit. Manuf.* 6 (2015) 39–52.
- [85] M.L. Griffith, M.E. Schlienger, L.D. Harwell, M.S. Oliver, M.D. Baldwin, M.T. Ensz, et al., Understanding thermal behavior in the LENS process, *Mater. Des.* 20 (2–3) (1999) 107–113.
- [86] D. Hu, R. Kovacevic, Sensing, modeling and control for laser-based additive manufacturing, *Int. J. Mach. Tools Manuf.* 43 (1) (2003) 51–60.
- [87] S. Karnati, N. Matta, T. Sparks, F. Liou, Vision-based process monitoring for laser metal deposition processes, 24th International Solid Freeform Fabrication Symposium; Austin, TX, 2013.
- [88] L. Tang, R.G. Landers, Melt pool temperature control for laser metal deposition processes: part I: online temperature control, *J. Manuf. Sci. Eng.* 132 (1) (2010).
- [89] F. Wang, H. Mao, D. Zhang, X. Zhao, Y. Shen, Online study of cracks during laser cladding process based on acoustic emission technique and finite element analysis, *Appl. Surf. Sci.* 255 (5, Part 2) (2008) 3267–3275.
- [90] Thermal imaging for assessment of electron-beam freeform fabrication (EBF3) additive manufacturing deposits, in: J.N. Zalameda, E.R. Burke, R.A. Hafley, K.M.B. Taminger, C.S. Domack, A. Brewer, et al., (Eds.), SPIE Proceedings, 8705, 2013 (Maryland, US).
- [91] S. Liu, W. Liu, M. Harooni, J. Ma, R. Kovacevic, Real-time monitoring of laser hot-wire cladding of Inconel 625, *Opt. Lasers Technol.* 62 (10) (2014) 124–134.
- [92] K. Bartkowiak, Direct laser deposition process within spectrographic analysis in situ, *Phys. Procedia* 5 (Part B) (2010) 623–629.
- [93] G.T. Loughnane, S.L. Kuntz, N. Klingbeil, J.M. Sosa, J. Irwin, A.R. Nassar, et al., Application of a microstructural characterization uncertainty quantification framework to Widmanstätten alpha-laths in additive manufactured Ti–6Al–4V, 26th International Solid Freeform Fabrication Symposium; Austin, TX, 2015.
- [94] L. Song, J. Mazumder, Real time Cr measurement using optical emission spectroscopy during direct metal deposition process, *IEEE Sensors J.* 12 (5) (2012) 958–964.
- [95] A.R. Nassar, T.J. Spurgeon, E.W. Reutzel, Sensing Defects During Directed-Energy Additive Manufacturing of Metal Parts Using Optical Emissions Spectroscopy, 25th International Solid Freeform Fabrication Symposium; Austin, TX, 2014.
- [96] A. Heralić, A.-K. Christiansson, B. Lennartson, Height control of laser metal-wire deposition based on iterative learning control and 3D scanning, *Opt. Lasers Eng.* 50 (9) (2012) 1230–1241.
- [97] T. Watkins, H. Bilheux, A. Ke, A. Payzant, R. Dehoff, C.E. Duty, et al., Neutron characterization for additive manufacturing, *Adv. Mater. Process.* 171 (3) (2013) 23–27.
- [98] T. Hutchings, P.J. Withers, T.M. Holden, T. Lorentzen, Introduction to the Characterization of Residual Stress by Neutron Diffraction, Taylor & Francis, 2004.
- [99] H.Z. Bilheux, R.L. McGreevy, I.S. Anderson, Neutron Imaging and Applications: A Reference for the Imaging Community, Springer Science and Business Media, LLC, New York, 2009.
- [100] A.S. Tremsin, J.B. McPhate, A. Steuwer, W. Kockelmann, M. Paradowska A, Kelleher JF, et al. high-resolution strain mapping through time-of-flight neutron transmission diffraction with a microchannel plate neutron counting detector, *Strain* 48 (4) (2012) 296–305.
- [101] S. Pierret, A. Evans, A.M. Paradowska, A. Kaestner, J. James, T. Etter, et al., Combining neutron diffraction and imaging for residual strain measurements in a single crystal turbine blade, *NDT&E Int.* 45 (1) (2012) 6.
- [102] M. Klein, J. Sears, Laser Ultrasonic Inspection of laser Cladded 316LSS and Ti-6-4, 23rd International Congress on Applications of Lasers and Electro-Optics, Orlando, Florida, Laser Institute of America, 2004.
- [103] R.S. Edwards, B. Dutton, A.R. Clough, M.H. Rosli, Scanning laser source and scanning laser detection techniques for different surface crack geometries, Review of Progress in Quantitative Nondestructive Evaluation; Burlington, VT: AIP Conference Proceedings 2012, pp. 251–258.
- [104] M. Klein, T. Sienicki, J. Eichenberger, Inventor slaser-ultrasonic detection of sub-surface defects in processed metals, United States 2007 4th October, 2005.
- [105] D. Clark, S.D. Sharples, D.C. Wright, Development of online inspection for additive manufacturing products, *Insight Non-Destr. Test. Cond. Monit.* 53 (11) (2011) 610–613.
- [106] D. Clark, D.C. Wright, Inventors Method of [sic] Producing an Object Including Testing and/or Analysing of Object, European 2009.
- [107] W. Li, J. Coulson, J.W. Aveson, R.J. Smith, M. Clark, M.G. Somekh, et al., Orientation characterisation of aerospace materials by spatially resolved acoustic spectroscopy, *J. Phys. Conf. Ser.* 520 (1) (2014).
- [108] R.J. Smith, W. Li, J. Coulson, M. Clark, M.G. Somekh, S.D. Sharples, Spatially resolved acoustic spectroscopy for rapid imaging of material microstructure and grain orientation, *Meas. Sci. Technol.* 25 (5) (2014).
- [109] S.O. Achamfuo-Yeboah, R.A. Light, S.D. Sharples, Optical detection of ultrasound from optically rough surfaces using a custom CMOS sensor, *J. Phys. Conf. Ser.* 581 (1) (2015).
- [110] N. Karthik, H. Gu, D. Pal, T. Starr, B. Stucker, High frequency ultrasonic non destructive evaluation of additively manufactured components, 24th International Solid Freeform Fabrication Symposium; Austin, TX: UT Austin, 2013.
- [111] H. Reider, A. Dillhöfer, M. Spies, J. Bamberg, T. Hess, Online Monitoring of Additive Manufacturing Processes Using Ultrasound 11th European Conference on Non-Destructive Testing, Czech Republic, Prague, 2014.
- [112] G. Georgeson, T. Edwards, J. Engel, D. Shedlock, X-ray Backscatter Imaging for Aerospace Applications, NASA, 2010.
- [113] S. Naito, S. Yamamoto, S. Yamamoto, Novel X-ray backscatter technique for detecting crack below deposit, 7th International Conference on NDE in Relation to Structural Integrity for Nuclear and Pressurized Components; 12th–15th May 2009; Yokohama, Japan, 2010.
- [114] D. Kayser, T. Bothe, W. Osten, Scaled topometry in a multisensor approach, *Opt. Eng.* 43 (10) (2004) 2469–2477.
- [115] E. Manske, T. Hausotte, R. Mastoylo, T. Machleidt, K.-H. Franke, G. Jäger, New applications of the nanopositioning and nanomeasuring machine by using advanced tactile and non-tactile probes, *Meas. Sci. Technol.* 18 (2) (2007) 520–527.
- [116] A. Weckenmann, X. Jiang, K.-D. Sommer, U. Neushaefer-Rube, J. Seewig, L. Shaw, et al., Multisensor data fusion in dimensional metrology, *CIRP Ann. Manuf. Technol.* 58 (1) (2009) 701–721.
- [117] J. Wang, R.K. Leach, X. Jiang, Review of the mathematical foundations of data fusion techniques in surface metrology, *Surf. Topogr. Metrol. Prop.* 3 (2) (2015).
- [118] J. Wang, X. Jiang, L.A. Blunt, R.K. Leach, P.J. Scott, Intelligent sampling for the measurement of structured surfaces, *Meas. Sci. Technol.* 23 (8) (2012).
- [119] R. Baranuik, More is less: signal processing and the data deluge, *Science* 331 (6018) (2011) 717–719.
- [120] D.A. Kriczky, J. Irwin, E.W. Reutzel, P. Michaleris, A.R. Nassar, J. Craig, 3D spatial reconstruction of thermal characteristics in directed energy deposition through optical thermal imaging, *J. Mater. Process. Technol.* 221 (7) (2015) 172–186.
- [121] K. Harding, Handbook of Optical Dimensional Metrology, Florida, Taylor & Francis Group, 2013 (506 p).
- [122] R.K. Leach, Optical Measurement of Surface Topography, Springer-Verlag, Berlin, 2011 (319 p).
- [123] M. Abolbashedari, A.S. Gerges, A. Davies, Dual Moiré and laser interferometry as a metrology tool, 27th ASPE Annual Meeting; San Diego, CA: Conference Proceedings 2012, pp. 256–259.